The charge ratio of the atmospheric muons at low energy

M. Bahmanabadi,[1,2,*] F. Sheidaei,[1] M. Khakian Ghomi,[2] and J. Samimi[1,2]

[1]*Department of Physics, Sharif University of Technology, P.O.Box 11365-9161, Tehran, Iran*

[2]*ALBORZ Observatory, Sharif University of Technology, Tehran, Iran*

(Received 22 October 2005; published 18 October 2006)

From the nature of the muon production processes, it can be seen that the ratio of positive to negative cosmic muons has important information in both ''the atmospheric neutrino problem,'' and ''the hadronic interactions.'' We have carried out an experiment for the measurement of the muon charge ratio in the cosmic ray flux in momentum range 0.112–0.178 GeV/c. The muon charge ratio is found to be 1.21 ± 0.01 with a mean zenith angle of $32° \pm 5°$. From the measurements it has been obtained a zenithal angle distribution of muons as $I(\theta) = I(0)\cos^n\theta$ with $n = 1.95 \pm 0.13$. An asymmetry has been observed in East-West directions because of the geomagnetic field. Meanwhile, in about the same momentum range, positive and negative muons have been studied on the basis of Monte Carlo simulations of the extensive air shower developement (Cosmic Ray Simulations for Kascade), using the Quark Gluon String model with JETs model as generator.

DOI: 10.1103/PhysRevD.74.082006 PACS numbers: 96.50.sd, 13.85.−t, 96.50.S−

I. INTRODUCTION

The primary cosmic rays hitting the top of the Earth's atmosphere are almost all protons or heavier atomic nuclei. These primary cosmic rays highly interact with the Earth's atmosphere and produce copious quantities of secondary particles. The most common secondary particles are baryons and mesons. The atmospheric flux of muons mainly originate from the decay of charged pions ($\tau_0 = 26$ ns) and kaons ($\tau_0 = 12$ ns) with branching ratios of $\sim$100% and $\sim$63.5% respectively. Muons have a much longer lifetime than pions and kaons. A muon has a mean lifetime of about $\tau_0 = 2.197$ μs, so it can reach the Earth before it decays: $\mu^{\pm} \rightarrow e^{\pm} + \nu_e(\bar{\nu}_e) + \bar{\nu}_\mu(\nu_\mu)$.

The muon charge ratio, $R = \mu^+/\mu^-$, is important in giving information about ''the atmospheric neutrino problem,'' and about ''the properties of hadronic interactions.'' The low energy muon flux is an important source of ν_e, $\bar{\nu}_e$, ν_μ, $\bar{\nu}_\mu$. The ratios $\nu_e/\bar{\nu}_e$ and $\nu_\mu/\bar{\nu}_\mu$ are directly related to the muon charge ratio. A rough addition of the flavors in the decay chains lead to the ratio:

$$R_\nu = \frac{\nu_\mu + \bar{\nu}_\mu}{\nu_e + \bar{\nu}_e} = 2. \quad (1)$$

Super-Kamiokande [1,2] and other experiments find that the ratio of muon neutrinos to electron neutrinos is significantly lower than the theoretical value $\sim$2 [3,4]. This anomaly has been explained in terms of neutrino oscillations($\nu_\mu \rightarrow \nu_\tau$) [1]. At the low energy range of muons ($\sim$ 1 GeV), the muon charge ratio is directly related to the number of electronic neutrinos and antineutrinos by $\mu^+/\mu^- = \nu_e/\bar{\nu}_e$ [4], and since neutrinos and antineutrinos interact with matter in different ways [5], the muon charge ratio can be important for the response of neutrino detectors. Therefore for exact analysis of the experiments related to the ratio R_ν, a precise knowledge of the contribution of each neutrino flavor is necessary. On the other hand, the muon charge ratio provides important information on the interactions of the primary cosmic rays with nuclei in the atmosphere. Thus, in addition to the particle physics aspects, there are further perspectives of muon charge ratio studies which contribute to a general knowledge of our environment. Meanwhile, since arrival directions of cosmic rays are essentially isotropic, the atmospheric flux of muons originating from the decay of charged pions and kaons produced by cosmic ray interactions in the atmosphere is nearly isotropic as well. Nevertheless, at lower muon energies it is influenced by the magnetic field of the Earth. Thus a detailed understanding of the asymmetries of the fluxes of positive and negative muons is indispensable for reliable calculations of the atmospheric neutrino flux. The muon charge ratio is a quantity rather sensitive to the effects of the geomagnetic field. Most of the previous measurements for obtaining the muon charge ratio have been carried out using magnetic deflection to determine the muon charge with simultaneous determinations of the energy [6–8]. The other experimental approach is the method of delayed coincidences [9,10]. The magnetic spectrometers are difficult to use for very low energy muons, due to presence of a large percentage of electrons in the secondary cosmic rays and different acceptances for positive and negative particles [11]. To avoid the difficulties and the systematic errors of magnetic spectrometers we use the method of delayed coincidences, which is based on the different interactions of positive and negative muons with matter. A cosmic ray telescope has been constructed for measuring the muon charge ratio at Sharif University of Technology in Tehran (35°43′N, 51°20′E). We used this method for determination of muon charge ratio. The elevation of the site is 1200 m above sea level (890 g cm^{-2}). The purpose of the experiment is investigation of the zenithal and azimuthal

*Electronic address: bahmanabadi@sina.sharif.edu

dependence of the muon charge ratio, and as a consequence the mean muon charge ratio is determined. We did the experiment with lower data in our previous paper [12], but in this paper we improved our previous results and have also used showers simulated by Cosmic Ray Simulations for Kascade (CORSIKA) to compare the measured results with simulation.

II. METHOD AND DATA ANALYSIS

When negative and positive muons are stopped in matter, they have different behaviors. The main idea of the delayed coincidence method is based on these behaviors. When a positive muon is stopped in scintillator or any other material, it always decays. But for negative muons there is an alternative reaction in the presence of matter. The host atom captures the negative muon and forms a "muonic atom" [13]. Since a muon is about 200 times more massive than an electron, its orbit can be very close to the nucleus and can often be captured by the nucleus. In fact, the negative muon interacts with atomic nuclei according to the reaction $\mu^- + p \rightarrow n + \nu_\mu$. Practically the entire energy librated in this process is carried off by the neutrino and no signal will be produced in the detector. As a result the mean negative muon lifetime becomes $1/\tau_{\mu^-} = \Lambda_c + 1/\tau_0$, where Λ_c is the capture probability and τ_0 the decay lifetime for a free muon. The nuclear capture rate is proportional to Z^4 and so becomes significant for sufficiently high Z atoms. Table I shows the mean lifetime and the decay probability of negative muon in some elements [14].

Thus, the muon charge ratio can be extracted from the measured decay curve, which is a superposition of the different lifetimes of negative muons in scintillator and the absorber material and decay of positive muons. If there are no backgrounds, the expected time spectrum is as

$$\frac{dN}{dt} = \frac{N_t}{R+1}\left[R\delta_0\frac{1}{\tau_0}\exp(-t/\tau_0) + \sum_j \delta_j \frac{1}{\tau_j} \times \exp(-t/\tau_j)\right], \quad (2)$$

where index 0 stands for positive muons, while the index $j(1, 2, 3, \ldots)$ indicates the negative muons decaying in the different absorber materials. $R = \mu^+/\mu^-$ represents the muon charge ratio, N_t is the total number of two muons, and the parameters δ_0 and δ_j include the stopping powers of different materials, the decay probability for the negative muons, and the efficiencies to detect the resulting electron or positron, which are determined by Monte Carlo simulation. We can split δ_j in the form of

$$\delta_j = S_j P^j_{\text{decay}}, \quad (3)$$

where only S_js are determined from the simulation and decay probabilities, P^j_{decay}, are taken from Table I. In order to reduce the number of free parameters of the fit, the mean lifetime and the probability of decay are extracted from Table I. By fitting Eq. (2) on our experimental data, N_t and R are obtained.

TABLE I. Mean lifetime and decay probability of negative muons in some elements.

	Mean lifetime(ns)	Decay probability(%)
Vacuum	2197.03 ± 0.04	100.00
Carbon	2026.3 ± 1.5	92.15
Oxygen	1795.4 ± 2	81.57
Aluminium	864.0 ± 1	39.05
Silicon	756.0 ± 1	34.14
Lead	75.4 ± 1	2.75

III. EXPERIMENTAL ARRANGEMENT

The block diagram of electronic apparatus and detectors is shown in Fig. 1. Three scintillators ($100 \times 14 \times 1$ cm^3) placed on top of each other were used to measure muon decay. The spacing of the top and bottom scintillators is 283 cm, and that of the middle and bottom scintillators is 10 cm. A 7 cm thick aluminum block was placed between the middle and bottom scintillators. Its operation is initiated when an incoming muon passes through the top and middle scintillators. The generated signals from the photomultiplier tubes viewing the scintillators are amplified in one stage ($\times$ 10) with a fast amplifier (CAEN N412). Then the signals are connected to an eight-channel fast discrim-

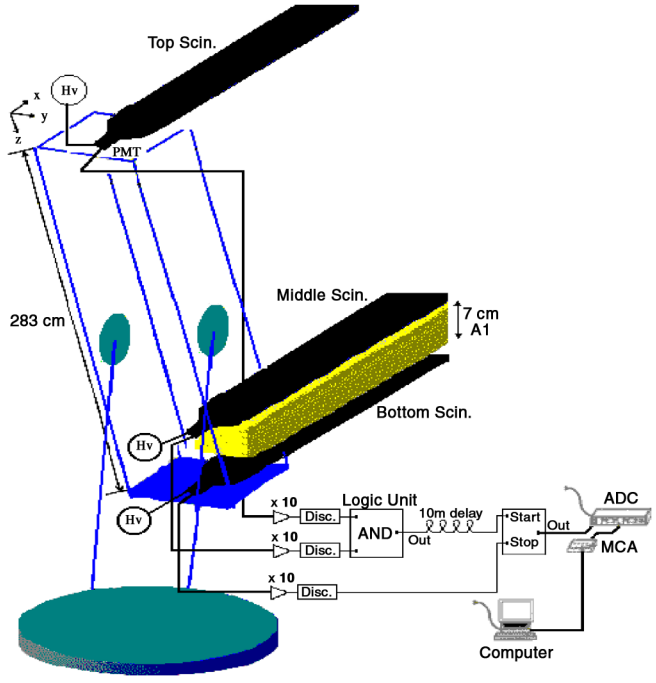

FIG. 1 (color online). Schematic view of detector, rotatable frame, and electronic circuit.

inator (CAEN N413A) which was operated at a fixed level of 20 mV. Each channel of the discriminator has two outputs; one of them is connected to a logic unit (CAEN N405) with a gate width of 150 ns. The output of the logic unit is connected to the start input of a time to amplitude converter (TAC, ORTEC 566) by a 10 m cable. The stopped muon in the aluminum or in the bottom scintillator decays at some later time. The neutrinos from the decay pass through the scintillator without any effect. The produced electron (positron) from the decay of the muon causes another signal in the bottom scintillator. This pulse through the amplifier and discriminator is sent to the stop input of the TAC. Finally the output of TAC, which was set to a full scale of 10 μs, is fed into a multichannel analyzer (MCA) via an analog to digital converter (ADC) unit. The time interval (Δt) between the start and stop signals is a measure of the muon lifetime. The length of the cable to the start input of the TAC is approximately 10 m longer than the length of the cable to the stop input. In its normal state, the TAC is ready to accept only a start pulse. It ignores the stop pulse, and the start pulse starts a timing run. The delay of the start pulse relative to the stop pulse corresponding to the 10 m of additional cable assures that the stop input is no longer activated when the pulse gets to the start input. The 10 m cable approximately reduces the time by 50 ns, and when corrected for it does not change the shape of the time spectrum stored and the mean lifetime obtained from the slope of the spectrum.

Our cosmic ray telescope is equipped for the measurement of zenith and azimuthal angular dependence of muon intensities. The calculated geometrical acceptance solid angle of the telescope is about 26 cm^2 sr.

IV. EXPERIMENTAL MEASUREMENTS AND RESULTS

We measured the decay spectrum of muons for 12 directions towards the North, West, South, and East each in three zenith angles of $20° \pm 10°$, $40° \pm 10°$, and $60° \pm 10°$. The momentum range of muons is 0.112–0.178 GeV/c. The measurements cover a total period of 1152 h. To compare the decay spectrum of different directions we changed pointing direction of the telescope while all the rest of the setup (including distances of

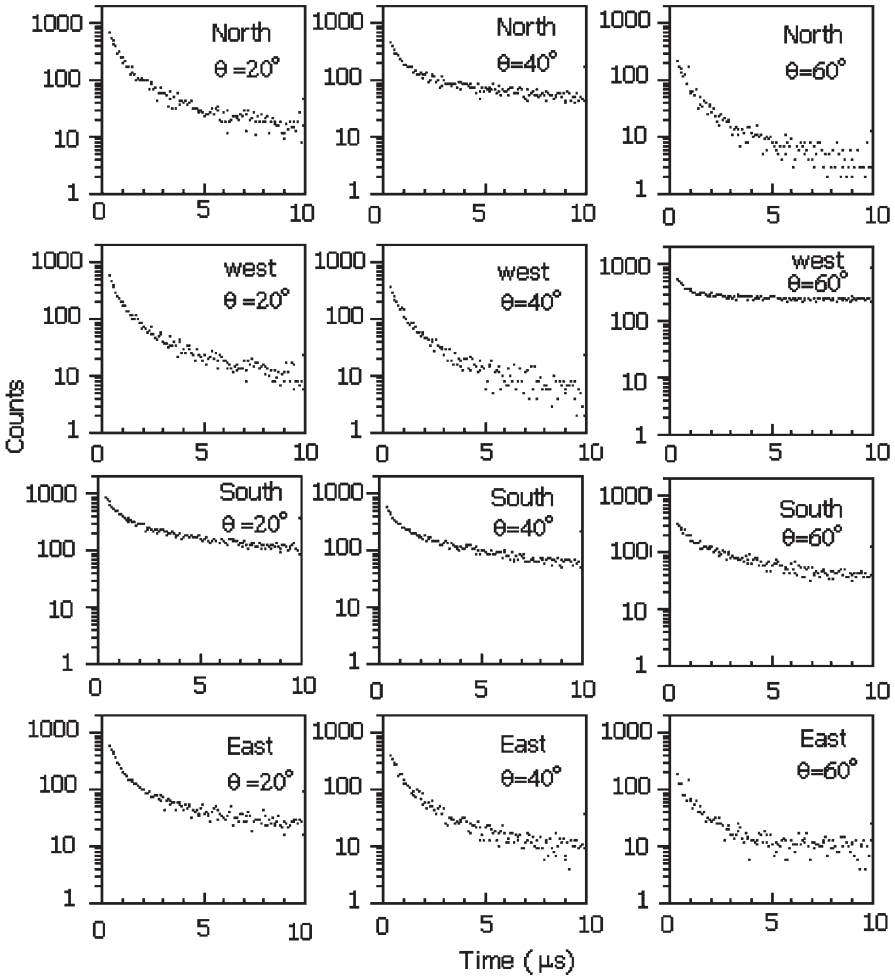

FIG. 2. Muon decay spectrum obtained from different directions.

scintillators, voltages, thresholds, etc.) were kept untouched and equal exposure times were used for different directions. Figure 2 shows the data obtained from different directions. By fitting the decay curve (Eq. (2)) on the data, N_t and R are determined. Note that Eq. (2) assumes that we are able to view the entire muon decay spectrum, whereas the circuit logic of the present experiment forces us to blank out the first 30 channels (~ 0.3 μs) of the muon spectrum. The omission of these channels weights slightly the positive muon component which has the longer lifetime. Thus we have a small systematic error in the use of Eq. (2). On the other hand, there is another exponential which is due to the background from random coincidences. Nevertheless, due to the long lifetime of this exponential, the background is approximately uniformly distributed in the time window of 10 μs. Figure 3 shows the data after background is subtracted. For all spectra the fit regression is more than 96%.

Figure 4 shows the differential zenith angle distribution of muons (N_t). The zenith angle distribution can be represented by $I(\theta) = I(0)\cos^n\theta$ with $n = 1.95 \pm 0.13$. Azimuthal angular dependence of muons can be seen in the μ^+/μ^- ratio in each zenithal angle. The errors of the ratio, 1 standard deviation σ, has been determined by the following equation:

$$\sigma = \frac{1}{N_-^2}\sqrt{N_+^2 N_- + N_+ N_-^2} = (1+R)\sqrt{R/N_t} \quad (4)$$

where N_+ and N_- show the number of positive and negative muons, $N_t = N_+ + N_-$, and $R = N_+/N_-$.

The muon charge ratio at various azimuthal angles is presented in Fig. 5, in the zenith angles $20° \pm 10°$, $40° \pm 10°$, and $60° \pm 10°$. The error bars show the statistical errors only. The results show a pronounced East-West effect in the low energy range, which is consistent with other previous results [15]. The reduction of the muon charge ratio in the east direction compared to the west, in the low energy range is thought to be caused by the geomagnetic effect. The azimuthal anisotropy, $A = (R_W - R_E)/(R_W + R_E)$, (with R_W and R_E being the values of the muon charge ratio measured in the west and east direction) is 0.12 in the momentum range 0.112–0.178 GeV/c, with a mean zenith angle $32° \pm 5°$. So the mean effective slant depth of the experiment is $X \simeq 890/\cos 32° = 1049$ g cm^{-2}, which is near the thickness of atmosphere at sea level.

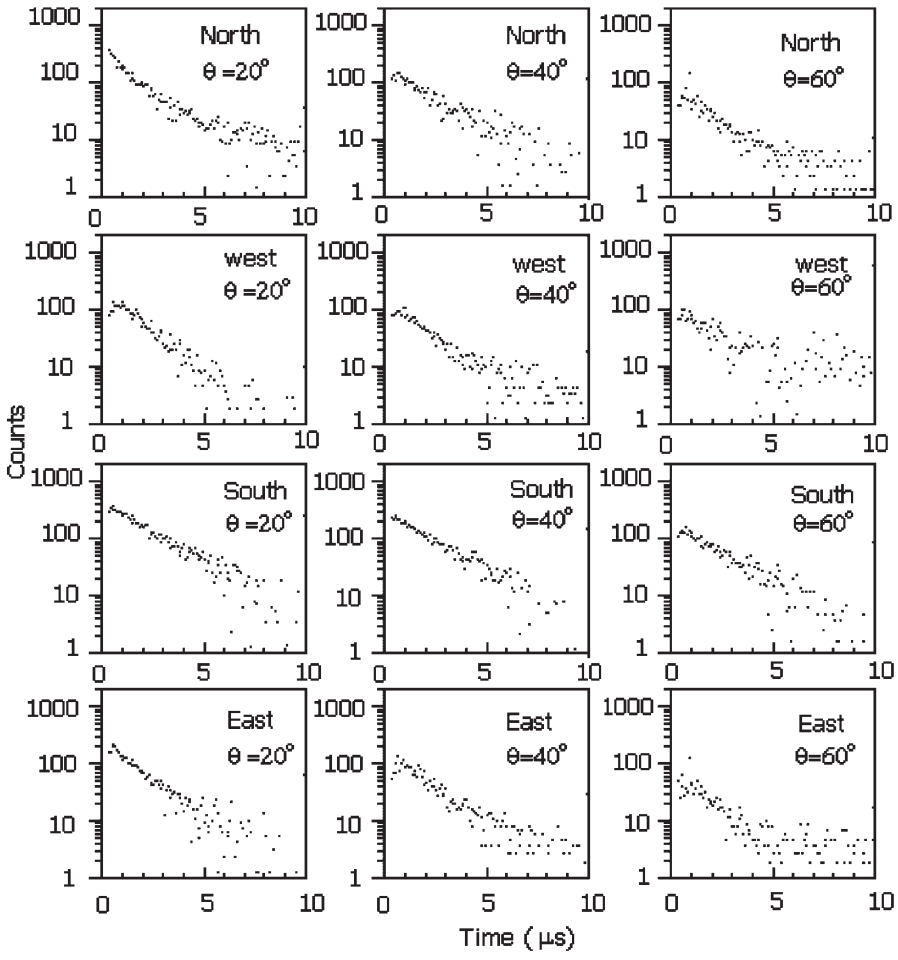

FIG. 3. Data after background is subtracted.

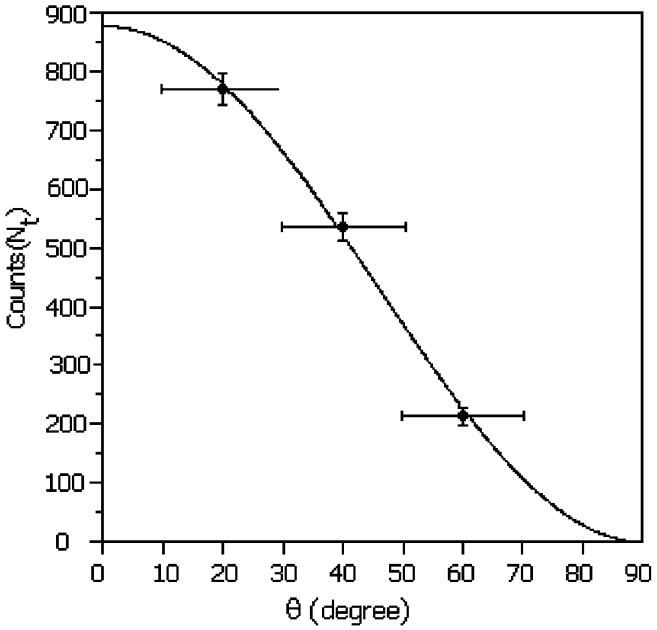

FIG. 4. The zenith angular dependence of muons. The smooth curve represents $N = N_\circ \cos^n\theta$ with $n = 1.95$.

A second experiment was carried out with the same telescope for muons arriving from the vertical direction. A 60 cm thick concrete block was placed above the top scintillator. This thickness of concrete is equivalent to about 150 g cm^{-2}. Our experiment has been done at 1200 m above sea level ($X_v = 890$ g cm^{-2}). Thus the total matter above our telescope is $890 + 150 = 1040$ g cm^{-2}, which is again near the thickness of atmosphere at sea level. The decay spectrum of muons obtained from this experiment is shown in Fig. 6 (a: the raw data, b: The data after subtracting background). More than 4×10^5 muons were accumulated by this experiment. From the measurements, we obtained $R = 1.21 \pm 0.01$.

The muon charge ratio results in the momentum range up to 10 GeV/c from the various experiments at sea level have been compiled in Fig. 7 [16–39], and our result has been shown with light circle.

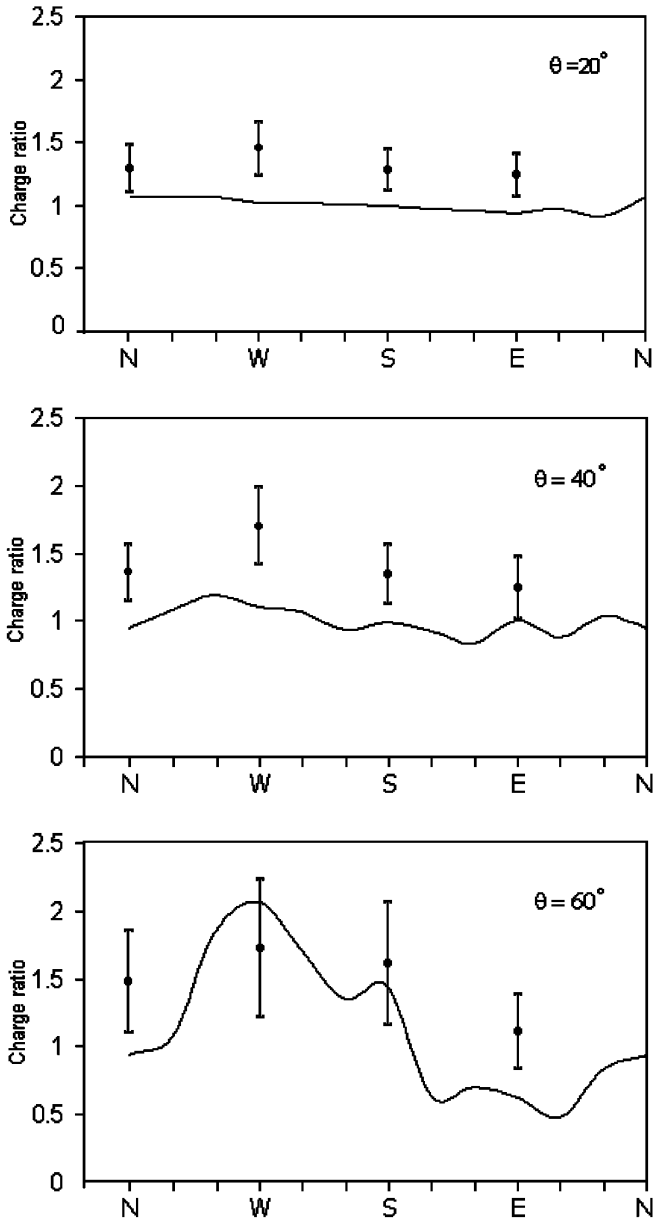

FIG. 5. The azimuthal angular dependence of the muon charge ratio for different zenith angles, compared with CORSIKA predictions (lines).

V. MONTE CARLO SIMULATION OF THE MUON FLUX

Atmospheric muons mainly originate from the interaction of particles in extensive air shower (EAS) events. These secondary muons are produced in the atmosphere by primary particles like gamma, proton, or heavier nuclei. But muon production of primary gamma photons with respect to primary nuclei, which are mostly protons, is very small. So we only investigated the primary nucleons and especially protons in our simulations. Cosmic ray muons observed with detectors placed at the ground level originate from the decay of mesons produced by interactions of high energy cosmic ray primaries with air nuclei, mainly due to the decay of charged pions and kaons. Pions and kaons have both decay and interaction in the atmosphere. Decay or interaction dominates depending on whether $\epsilon = \frac{mc^2 h_\circ}{c\tau}$ or E is larger [40] where m, c and τ are meson mass, the speed of light, and mean lifetime, respectivley, $h_\circ = 6.4$ km, and E is energy of meson. In the limit that $E \ll \epsilon$, interaction can be neglected [40]. The value ϵ for pion and kaon is 115 GeV and 850 GeV, respectively. So for low energies the limit is valid, and interaction can be neglected. In the EASs there are a large number of interactions of the following kinds which produce muons:

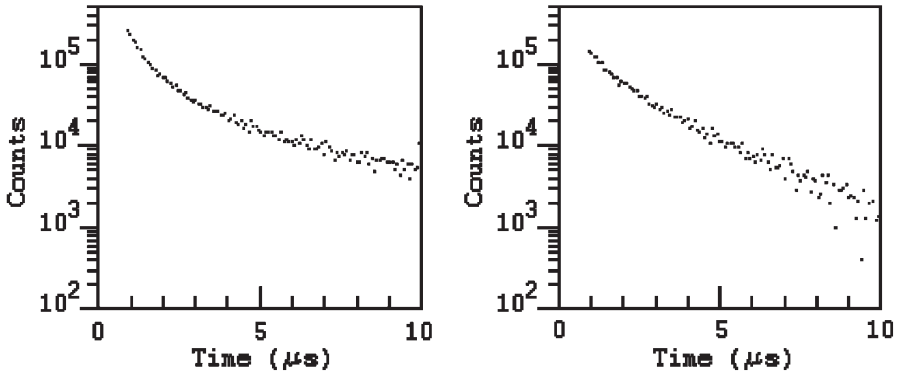

FIG. 6. Raw spectrum of muon decay (a), and subtracted background (b) in vertical direction along with a concrete block above the top scintillator.

$$A_{\mathrm{CR}} + A_{\mathrm{Air}} \rightarrow \pi^{\pm}, \pi^{0}, k^{\pm}, \quad \text{other hadrons} \tag{5}$$

$$\pi^{\pm} \rightarrow \mu^{\pm} + \nu_{\mu}(\bar{\nu}_{\mu}) \sim 100\% \qquad \tau_0 = 26 \text{ ns} \tag{6}$$

$$k^{\pm} \rightarrow \mu^{\pm} + \nu_{\mu}(\bar{\nu}_{\mu}) \sim 63.5\% \qquad \tau_0 = 12 \text{ ns} \tag{7}$$

Usually the produced muons in the EASs do not multiply, but only lose their energy slowly by ionization as they traverse in the atmosphere. The muon content of a shower increases up to a maximum and then attenuates very slowly. This is quite different from the electron component which attenuates relatively rapidly after maximum. So for the production of 0.112–0.178 GeV/c muons the lowest energy of primary particles is about a few GeVs or 10 GeVs. Therefore the study of the muon component of the EASs in the investigation is very important, especially for higher energy primaries. Since our experiment has been setup at the ALBORZ observatory located in Tehran, Iran,(35°43′N, 51°20′E) at 1200 m a.s.l corresponding to an average vertical atmospheric depth of 890 g cm^{-2}, the EASs were simulated utilizing the CORSIKA package [41] for investigation of the muon component. CORSIKA simulates EASs initiated by photons, protons, nuclei, or any other particle. Different hadronic interaction models are available in CORSIKA. Present results have been obtained by coupling the QGSJET- model (qgsjet01.f package) [42], for hadronic interactions above $E_{\mathrm{lab}} > 80$ GeV, and GHEISHA (Gamma Hadron Electron Interaction SHower code) [43] for interactions below this energy. The values of geomagnetic field components for Tehran ($B_x = 28.06\ \mu$T, $B_z = 38.37\ \mu$T) were obtained from the U.S. Geomagnetic Data Center [44]. The values of geomagnetic field are constant and independent of zenith and azimuthal angle of the muon. To illustrate this point we consider the relation between vertical altitude of atmosphere, h_v, and distance up the trajectory, l, is (for $l/R_{\oplus} \ll 1$) (Fig. 8)

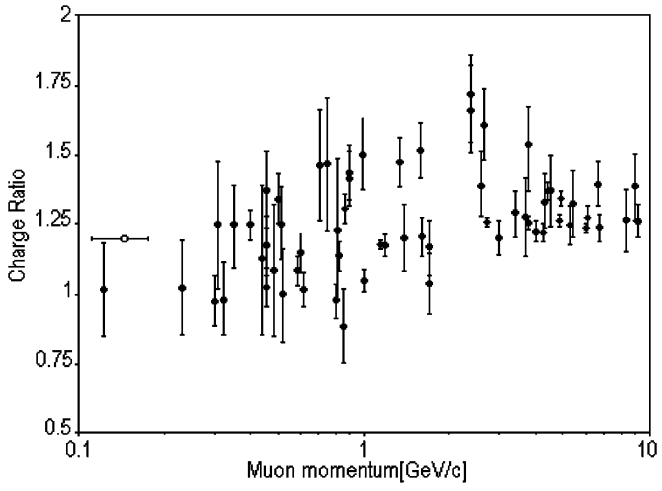

FIG. 7. Compilation of some selected measurements on the muon charge ratio in the momentum range up to 10 GeV/c [16–39]. Open circle shows our measurement.

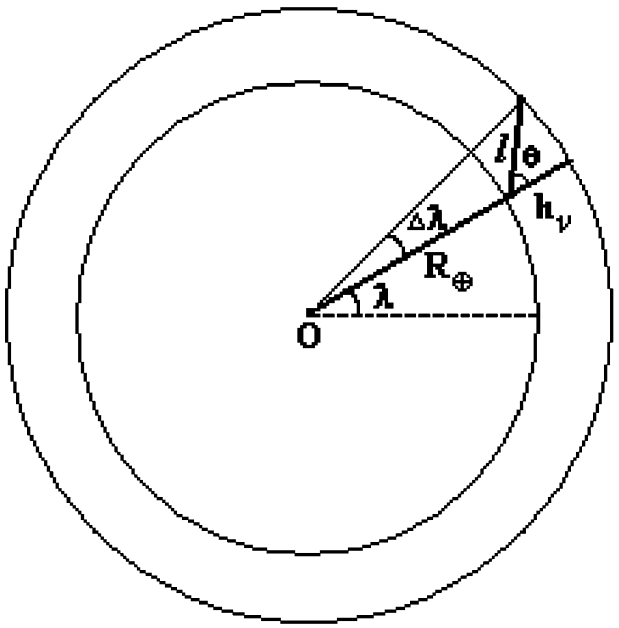

FIG. 8. A schematic of the Earth and atmosphere for showing the angles and notations used in the text.

$$h_v \simeq l\cos\theta + \frac{1}{2}\frac{l^2}{R_\oplus}\sin^2\theta. \quad (8)$$

For $\theta \leq 60^\circ$ the second term in (8) can be neglected. So to use the sine rule, $\Delta\lambda$ is obtained

$$\frac{\sin\Delta\lambda}{l} = \frac{\sin\theta}{R_\oplus + h_v}. \quad (9)$$

Using $l = h_v/\cos\theta$, $\theta = 60^\circ$, $h_v \simeq 20$ km, and $R_\oplus = 6400$ km, the value $\Delta\lambda$ is 0.3°. With this value $\Delta\lambda$, we calculated the relative variation of geomagnetic field components in Tehran. To assume the geomagnetic field as a dipole we obtain $|\frac{\Delta B_x}{B_x}| = 0.003$ and $|\frac{\Delta B_z}{B_z}| = 0.007$. These errors are relatively small, and so the uniform field is a good assumption. The range of energy for primary particles was selected from 5 GeV to 5 PeV, with differential flux given by $dN/dE \propto E^{-2.7}$. These simulations were carried out for different directions, with zenith angle in bins 0–10°, 10°–20°, ..., and 60°–70°; and in each 10° zenith angle interval all azimuth angles. Since the greatest contribution of the produced muons is from protons and alpha particles, we simulated only these two kinds of particles and then weighted to their measured compositions. We assumed an isotropic distribution for the incoming particles at the top of the atmosphere. We selected muons with momentum values between 0.1 GeV/c to 0.5 GeV/c in these simulations, which is near the momentum range of our experiment. In Fig. 5 the CORSIKA predictions of the muon change ratio have been compared with the experimental data. A distinguished East-West asymmetry effect, with an anisotropy value $A = 0.27$, is also seen from the simulation results.

One can recognize that for measurements with small zenith angles, the simulations generate values consistently smaller than the measured results for low energy (less than 1 GeV) muons. The smaller simulated value of the charge ratio at very low energies is associated with peculiarities of the interaction models.

The results of the CORSIKA simulations in this momentum range give a mean value of 1.02 for muon charge ratio with a mean zenith angle of $\sim 30^\circ$.

VI. CONCLUDING REMARKS

A cosmic ray detector has been installed at Sharif University of Technology in Tehran for the study of the muon charge ratio. By applying the method of delayed coincidences, we determined the charge ratio of cosmic ray muon in momentum range 0.112–0.178 Gev/c. In this experiment we used aluminum for an efficient separation of the two types of muons. Our measurements indicate a muon charge ratio value of 1.21 ± 0.01 with a mean zenith angle of $32^\circ \pm 5^\circ$. An East-West asymmetry effect is observed at low energy, which is due to the geomagnetic field. The East-West asymmetry effect can be shown by the quantity $A = (R_W - R_E)/(R_W + R_E)$ which has been found to be 0.12 in the momentum range 0.112–0.178 GeV/c. We have also found that the zenith angle of the arrival direction of muons obeys a $\cos^n\theta$ law with $n = 1.95 \pm 0.13$ in this momentum range.

The simulation results with CORSIKA confirm the East-West asymmetry effect found in the muon charge ratio measurements with an anisotropy value of $A = 0.27$. For vertical measurement the CORSIKA simulation gives smaller results than the measurements. This smallness of the charge ratio at very low energies could be associated with peculiarities of the interaction models. This study opens a field of interest in view of improving different interaction models, e.g., CHEISHA, which is dedicated for the low energy regions, and needs careful theoretical and experimental investigations. Muon charge ratio spectroscopy has an interesting information potential for several problems: about hadronic interactions and about the ratio of electron- antineutrinos to electron- neutrinos in the atmospheric flux. The analysis of the simulation results leads to $R = 1.02$ in momentum range 0.1–0.5 GeV/c with a mean zenith angle of $\sim 30^\circ$.

ACKNOWLEDGMENTS

This research has been partly supported by Grant No. NRCI 1853 of the National Research Council of Islamic Republic of Iran.

[1] Y. Fukuda *et al.*, Phys. Rev. Lett. **81**, 1562 (1998); Phys. Lett. B **436**, 33 (1998).
[2] K. S. Hirata *et al.*, Phys. Lett. B **205**, 416 (1988).
[3] T. K. Gaisser and T. Stanev, Phys. Rev. D **38**, 85 (1988).
[4] M. Honda *et al.*, Phys. Rev. D **52**, 4985 (1995).
[5] P. Lipari, Astropart. Phys. **1**, 195 (1993).
[6] G. Basini, Proc. 22th ICRC, Dublin, Ireland **HE 4.1.5**, 544 (1991).
[7] S. A. Stephens and R. L. Golden, Proc. 20th ICRC, Moscow, Russia **6**, 173 (1987).
[8] G. Tarle *et al.*, Proc. 25th ICRC, Durban, South Africa **6**, 321 (1997).
[9] C. P. Achenbach and J. H. Cobb, Proc. 27th ICRC, Hamburg, Germany **HE274**, 1313 (2001).
[10] I. M. Brancus *et al.*, Proc. 27th ICRC, Hamburg, Germany **HE216**, 944 (2001).
[11] B. Volpescu *et al.*, Forschungszentrum Karlsruhe Report No. FZKA6071, 1998 (unpublished).
[12] M. Bahmanabadi, M. khakian Ghomi, and F. Sheidaei Astropart. Phys. **24**, 183 (2005).

[13] J. Hufner, F. Scheck, and C. S. Wu, in *Muon Physics*, edited by V. W. Hughes and C. S. Wu (Academic Press., New York, 1977).
[14] T. Suzuki, D. F. Measday, and J. P. Roalsvig, Phys. Rev. C **35**, 2212 (1987).
[15] S. Tsuji *et al.*, Proc. 26th ICRC, Salt Lake City, Utah, USA **2**, 52 (1999).
[16] M. Conversi, Phys. Rev. **79**, 749 (1950).
[17] B. G. Owen and J. G. Wilson, Proc. Phys. Soc. London, Sect. A **64**, 417 (1951).
[18] J. R. Moroney and J. K. Parry, Aust. J. Phys. **7**, 424 (1954).
[19] S. Fukui, J. Phys. Soc. Jpn. **10**, 735 (1955).
[20] J. E. R. Holmes, B. G. Owen, and A. L. Rodgers, Proc. Phys. Soc. London **78**, 505 (1961).
[21] P. J. Hayman and A. W. Wolfendale, Nature (London) **195**, 166 (1962).
[22] D. W. Coates and W. F. Nash, Aust. J. Phys. **15**, 420 (1962).
[23] B. C. Rastin *et al.*, Proc. of the 9th ICRC **2**, 981 (1965).
[24] S. Kawaguchi *et al.*, Proc. of the 9th ICRC **2**, 941 (1965).
[25] O. C. Allkofer, R. D. Andresen, and W. D. Dau, Can. J. Phys. **46**, S301 (1968).
[26] S. R. Baber, W. F. Nash, and B. C. Rastin, Nucl. Phys. B **4**, 549 (1968).
[27] O. C. Allkofer and K. Klausen, Acta Physica Academiae Scientiarum Hungaricae **2**, 698 (1970).
[28] I. C. Appleton, M. T. Hogue, and B. C. Rastin, Nucl. Phys. B **26**, 365 (1971).
[29] O. C. Allkofer and W. D. Dau, Phys. Lett. B **38**, 439 (1972).
[30] M. S. Abdel-Monem *et al.*, Proc. of the 13th ICRC **3**, 1811 (1973).
[31] M. G. Thompson *et al.*, Proc. of the 13th ICRC **3**, 1822 (1973).
[32] T. H. Burnett *et al.*, Phys. Rev. Lett. **30**, 937 (1973).
[33] B. C. Rastin, J. Phys. G **10**, 1629 (1984).
[34] K. P. singhal, Proc. of the 18th ICRC **7**, 27 (1983).
[35] E. Schneider *et al.*, Proc. of the 24th ICRC **1**, 690 (1995).
[36] G. Basini *et al.*, Proc. of the 24th ICRC **1**, 585 (1995).
[37] J. F. Krizmanic *et al.*, Proc. of the 24th ICRC **1**, 593 (1995).
[38] W. Grandegger, Kernforschungszentrum-Karlsruhe Report No. 5122, 1993 (unpublished).
[39] T. E. Jannakos, Kernforschungszentrum-Karlsruhe Report No. 5520, 1995 (unpublished).
[40] T. K. Gaisser, *Cosmic Rays and Particle Physics* (Cambridge Univ. Press, New York, 1990).
[41] D. Heck *et al.*, Forschungszentrum Karlsruhe Report No. FZKA6019, 1998 (unpublished).
[42] N. N. Kalmykov and S. S. Ostapchenko, Yad. Fiz. **56**, 105 (1993) [Phys. At. Nucl. **56 N3**, 346 (1993)]; N. N. Kalmykov and S. S. Ostapchenko, and A. I. Pavlov, Bull. Acad. Sci. USSR, Phys. Ser. (English Transl.) **58 N12**, 21 (1994) [Bull. Acad. Sci. USSR, Phys. Ser. (English Transl.) **58**, 1966 (1994)]; Nucl. Phys. B, Proc. Suppl. **52B**, 17 (1997).
[43] H. Fesefeldt (GHEISHA), RWTH Aachen, Germany Report No. PITHA-85/02, 1985 (unpublished).
[44] http://www.ngdc.noaa.gov/seg/potfld/geomag.html (2002).